

Fluorescence XAFS Study on Local Structure around Cr Atoms Doped in ZnTe

Hironori Ofuchi¹, Nobuhiko Ozaki², Nozomi Nishizawa, Hidekazu Kinjyo², Shinji Kuroda², Koki Takita²

1 Japan Synchrotron Radiation Research Institute (JASRI), 1-1-1 Kouto, Sayo-cho, Sayo-gun, Hyogo, 679-5198, Japan

2 Institute of Materials Science, University of Tsukuba, 1-1-1 Tennoudai, Tsukuba, Ibaraki 305-8573, Japan

Abstract. The geometric structures for ferromagnetic $Zn_{1-x}Cr_xTe$ films grown by molecular beam epitaxy were investigated by fluorescence XAFS measurements in order to elucidate the relationship between the geometric structure and the magnetic properties. XAFS analysis suggested that the majority of Cr atoms doped in CrTe substituted the Zn-site in the ZnTe lattice below the Cr content $x = 0.048$, and formed Cr-Te compounds such as Cr_2Te_3 and CrTe above $x = 0.090$. It is suggested that ferromagnetism of the $Zn_{1-x}Cr_xTe$ films above $x = 0.090$ is due to the formation of Cr-Te compounds.

Keywords: diluted magnetic semiconductor, $(Zn,Cr)Te$, EXAFS

PACS: 78.70.Dm, 78.66.Hf, 68.55.Jk, 75.50.Pp

INTRODUCTION

For the last decade, diluted magnetic semiconductors (DMS's), which combine semiconductors and magnetism, have been extensively studied from the perspective of using spin degrees of freedom in semiconductor devices [1]. Recently, ferromagnetic behaviors were observed in $Zn_{1-x}Cr_xTe$ with Cr contents x reaching a few percent [2], and then the room-temperature ferromagnetism was reported in $Zn_{1-x}Cr_xTe$ in $x = 0.20$ [3]. However, the origin of the ferromagnetic transition in highly Cr-doped ZnTe is not yet fully understood.

In the present work, $(Zn,Cr)Te$ films grown by molecular-beam epitaxy (MBE) were investigated by fluorescence x-ray absorption fine structure (XAFS) measurements using synchrotron radiation in order to

elucidate the relationship between the local structures around the Cr atoms and the magnetic properties.

EXPERIMENTAL

The $(Zn,Cr)Te$ films were grown by the conventional MBE. Details of the growth process were described previously [4]. A ZnTe buffer layer was grown on a GaAs(001) substrate and then a $(Zn,Cr)Te$ layer with a thickness about 300 nm was grown on this buffer layer. The features of the samples are summarized in Table 1. The Cr composition was measured by electron probe microanalyzer (EPMA). Magnetic properties was investigated by superconducting quantum interference device (SQUID).

The EXAFS measurements were performed at the

TABLE 1. List of $Zn_{1-x}Cr_xTe$ films used in this study with Cr concentration, Curie temperature, and results of XRD. [Cr] were determined by EPMA.

Samples	Cr content : x [%]	Curie temperature : Tc [K]	XRD measurements
#A	0.009	5	$(Zn,Cr)Te$
#B	0.048	30	$(Zn,Cr)Te$
#C	0.090	125	$(Zn,Cr)Te$
#D	0.173	275	$(Zn,Cr)Te$
#E	0.414	318	$(Zn,Cr)Te$ and Cr_2Te_3 (or CrTe)

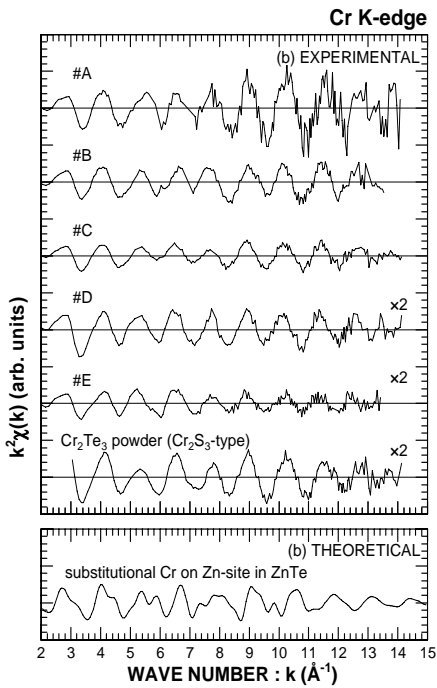


FIGURE 1. Cr K-edge EXAFS oscillation functions $k^2\chi(k)$ spectra for (a) $Zn_{1-x}Cr_xTe$ films and Cr_2Te_3 powder, (b) theoretical EXAFS spectrum for the substitutional Cr atom on the Zn-site in the ZnTe lattice. The Debye-Waller factor was assumed as 0.05 Å for the bond length below 4.0 Å and 0.075 Å for the bond length above 4.0 Å. The theoretical EXAFS spectrum was generated by FEFF8.

beam line BL12C at the Photon Factory in Tsukuba with a Si(111) double crystal monochromator and a bent cylindrical mirror using synchrotron radiation from the 2.5 GeV storage ring [5]. The EXAFS spectra were measured in the fluorescence-detection mode. The intensity of the incident X-ray beam was monitored by a nitrogen-filled ionization chamber, while the X-ray fluorescence signal was detected by an array of 19 elements of Ge solid state detectors. All the XAFS measurements were performed at 70 K in order to reduce thermal vibration.

RESULTS AND DISCUSSION

Figure 1 shows the Cr K-edge $k^2\chi(k)$ EXAFS spectra for the $Zn_{1-x}Cr_xTe$ samples and Cr_2Te_3 powder. It is found that the amplitudes of the EXAFS spectra decrease with increasing Cr content of the $Zn_{1-x}Cr_xTe$ samples, while the periods of the EXAFS spectra are almost the same. Figure 2 shows the Fourier transformed Cr K-edge EXAFS spectra for the $Zn_{1-x}Cr_xTe$ samples and Cr_2Te_3 powder. For all the samples, striking main peaks were observed at 2.5 Å.

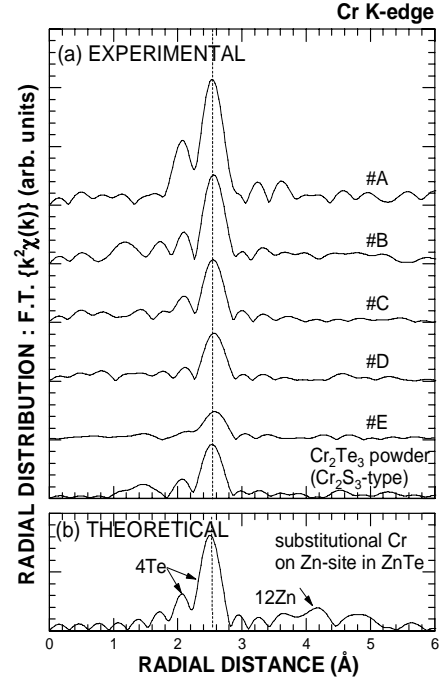


FIGURE 2. Fourier transform of Cr K-edge EXAFS oscillation functions $k^2\chi(k)$ spectra for (a) $Zn_{1-x}Cr_xTe$ films and Cr_2Te_3 powder, (b) theoretical EXAFS spectrum for the substitutional Cr atom on the Zn-site in the ZnTe lattice. The Fourier transformation was performed in the k range of 3.0 – 13.0 Å⁻¹. The Debye-Waller factor was assumed as 0.05 Å for the bond length below 4.0 Å and 0.075 Å for the bond length above 4.0 Å. The theoretical EXAFS spectra were generated by FEFF8.

The height of the main peaks decreases with increasing Cr content. Shift of the main peaks is not observed for each sample. The feature of the main peaks in the Cr_2Te_3 powder resembles that of the substitutional model in Fig. 2(b). Thus, it is difficult to deduce whether the $Zn_{1-x}Cr_xTe$ samples form the substitutional structure or Cr_2Te_3 from Fig. 2.

In order to get the details of the measured EXAFS spectra, parameter fitting was conducted with the theoretically generated spectra. The curve-fitting was carried out with theoretically calculated spectra using FEFF8 [6]. Figure 3 shows structural parameters which were obtained by the curve-fitting. For the $Zn_{1-x}Cr_xTe$ samples except #E, substitutional model was fitted best. Obtained coordination numbers are close to 4, which coincides with that for the substitutional model. Thus, it is expected that the majority of Cr atoms doped in the samples below the Cr content $x = 0.173$ substitute in the Zn-site in the ZnTe lattice. However, it is found that for the Cr_2Te_3 powder the substitutional model is also fitted well, although Cr_2Te_3 forms a Cr_2S -type structure. Therefore, it is difficult to distinguish between the

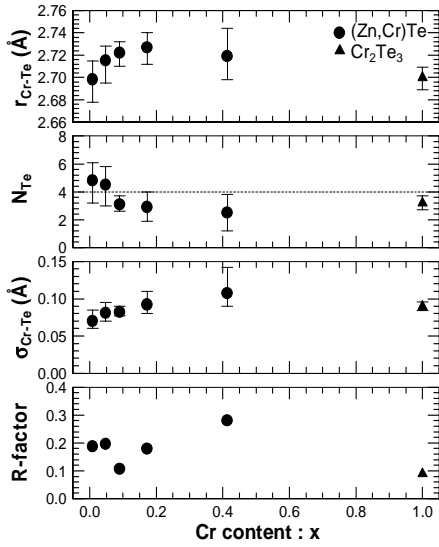


FIGURE 3. Variation of the bond length ($r_{\text{Cr-Te}}$), coordination number (N_{Te}), Debye-Waller factor ($\sigma_{\text{Cr-Te}}$), and R-factor versus Cr content (x). F-factor is the discrepancy index defined as

$$\text{R - factor} = \frac{\int |\chi_E(k) - \chi_T(k)| k^2 dk}{\int |\chi_E(k)| k^2 dk}, \text{ where } \chi_E \text{ and } \chi_T \text{ are}$$

the experimental and theoretical EXAFS, respectively.

substitutional and Cr_2S -type structure by EXAFS analysis.

Figure 4 represents Cr K-edge XANES spectra for $\text{Zn}_{1-x}\text{Cr}_x\text{Te}$ films and Cr_2Te_3 powder. Compared to each spectrum, it is found that the spectral features are divided into two types. For the samples #A and #B, the small ridges indicated by arrow were observed at 6.000 keV. On the other hand, for the samples #C, #D, and #E, no ridge was observed at 6.000 keV, which resembles that for the Cr_2Te_3 powder. The XRD results showed that the sample #E contained Cr_2Te_3 and/or CrTe compounds. Thus, it is expected that the samples #C, #D also contain the Cr-Te compounds such as Cr_2Te_3 and CrTe, although for the samples #C and #D Cr-Te compounds were not observed by XRD.

The XAFS results suggest that for the samples below a Cr content of $x = 0.048$ the majority of Cr atoms substituted in the Zn-site of the ZnTe lattice, and for the samples above $x = 0.090$ the Cr atoms forms Cr-Te compounds. Cr_2Te_3 and $\text{Cr}_{0.88}\text{Te}$ show ferromagnetism with $T_c = 322$ K and 354 K, respectively [7,8]. Thus, it is suggested that the ferromagnetism for the samples above $x = 0.090$ is due to the formation of Cr-Te compounds.

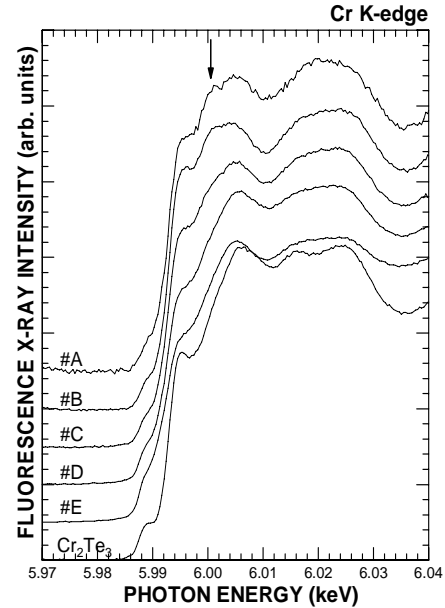


FIGURE 4. Cr K-edge XANES spectra for $\text{Zn}_{1-x}\text{Cr}_x\text{Te}$ films and Cr_2Te_3 powder.

ACKNOWLEDGMENTS

XAFS studies were performed as part of a project (Project No. 2005G181) accepted by the Photon Factory Program Advisory Committee.

REFERENCES

1. H. Ohno, *Science* **281**, 951-956 (1998).
2. H. Saito, V. Zayets, S. Tamagata, and K. Ando, *Phys. Rev. B* **66**, 1-4(0811201(R)) (2002).
3. H. Saito V. Zayerts, S. Yamagata, and K. Ando, *Phys. Rev. Lett.* **90**, 1-4 (2002).
4. S. Kuroda, N. Ozaki, N. Nishizawa, T. Kumekawa, S. Marcat and K. Takita, *Sci. Tech. Adv. Mater.* **6**, 558-564 (2005).
5. M. Nomura and A. Koyama, KEK Report **95-15** (1996).
6. A. L. Ankudinov, and J. J. Rehr, *Phys. Rev. B* **65**, 1-11(104107) (2002).
7. G. Peix, D. Babot and M. Chevreton, *J. Sol. Stat. Chem.* **36**, 161-170 (1981).
8. S. Ohta, S. Kurosawa, and S. Anzai, *J. Phys. Soc. Jpn.* **51**, 1386-1393 (1981).